Synthesis and Thermodynamic Properties of Poly(cyclohexylethylene-*b*-dimethylsiloxane-*b*-cyclohexylethylene)

Sudeep Maheshwari, Michael Tsapatsis, and Frank S. Bates*

Department of Chemical Engineering and Materials Science, University of Minnesota, Minneapolis, Minnesota 55455

Received May 19, 2007; Revised Manuscript Received July 10, 2007

ABSTRACT: Poly(styrene-*b*-dimethylsiloxane-*b*-styrene) (PS−PDMS−PS) triblock copolymers were prepared by anionic polymerization and subsequently hydrogenated using a platinum/rhenium catalyst supported on ultrawide pore silica (Pt/Re−SiO_2), yielding PCHE−PDMS−PCHE, where PCHE refers to poly(cyclohexylethylene). The hydrogenation reaction resulted in polymer with negligible chain degradation as confirmed by ^{1}H NMR and size exclusion chromatography (SEC). Small-angle X-ray scattering (SAXS) and transmission electron microscopy (TEM) experiments revealed a lamellar morphology for all specimens. Thermodynamic properties were inferred from the order−disorder transition temperatures as determined by SAXS and dynamical mechanical spectroscopy (DMS). The resulting segment−segment interaction parameter, $\chi(T)$, is assessed in the context of current published approaches to treating the thermodynamics of nonpolar polyolefins, particularly block copolymers.

Introduction

Polyolefins are commercially important polymers that constitute a major share of the plastics industry.[1] With the development of poly(cyclohexylethylene) (PCHE),[2] obtained by the hydrogenation of polystyrene, a new material was added to the existing library of these polymers. PCHE brings a plethora of interesting properties such as high modulus, high application temperature, and excellent optical properties.[1,3] A successful method for hydrogenating polystyrene (PS) without degradation was demonstrated by Gehlsen and Bates more than a decade ago.[2] However, application of that approach requires large amounts of catalyst, making this process uneconomical. At about the same time, Hucul and Hahn[3] developed a significantly more efficient hydrogenation catalyst by depositing platinum and other transition metals (e.g., rhenium) within a macroporous (ca. 300 nm pore diameter) silica substrate. This new catalyst permits nearly complete hydrogenation (>99%) of polystyrene without chain degradation, at overall loadings (metal and support) of about 0.07 g of the catalyst per gram of the polymer. Moreover, this catalyst can be regenerated for repeated use, making polystyrene hydrogenation a commercially viable process. However, PCHE homopolymer is a very brittle material, which further stalled its commercialization. Over the past 10 years, various studies have shown that this key limitation can be overcome through block copolymerization of PCHE with rubbery or semicrystalline polymers, including poly(ethylene), poly(ethylenepropylene), poly(ethylethylene), and combinations of these saturated hydrocarbons.[4−7] This report describes the synthesis and preliminary characterization of a new class of PCHE based block copolymers, obtained by catalytically hydrogenating PS−PDMS−PS triblock copolymers, where PS and PDMS denote poly(styrene) and poly(dimethylsiloxane), respectively. Remarkably, this saturation reaction results in almost no chain degradation, thus permitting us to evaluate the morphology and mixing thermodynamics of this pair of nonpolar polymers.

The thermodynamics of polymer−polymer mixing dictate the phase behavior of homopolymer blends and the morphology of block copolymers. Anticipating the magnitude of the segment−segment interactions that govern pairs of macromolecules, particularly polyolefins, continues to represent a theoretical challenge. Polyolefin blends and block copolymers are rather weakly interacting systems, governed by relatively small interaction parameters, $\chi \sim O(10^{-2})$. As a consequence, nonregular factors, such as system compressibility and excess entropic contributions associated with complex, nonideal segment packing, can have a decisive influence over the phase behavior of these materials. Over the past few years, a host of experimental and theoretical studies[2,8−26] have addressed these and other noncombinatorial contributions to the overall mixing free energy, expanding our understanding of polymer mixing thermodynamics.

Additional perplexing phenomena have been reported in the past decade or so, showing that the phase behavior of binary polymer mixtures and block copolymers is far richer than previously thought. For example, the influence of pressure on mixing or demixing has been reported in certain polyolefin systems.[27−30] Interestingly, depending on the particular pair of polyolefins and the pressure, mixing can be enhanced or reduced with increasing pressure. Disorder (homogeneous) to order (microphase separated) transitions (LDOT) have been reported upon heating in some of these weakly interacting block copolymer systems,[31−33] contrary to the predictions of the well-established mean-field theories.[16] Very recently, closed loop phase behavior has been observed with poly(styrene−pentyl methacrylate) diblock copolymers,[34−36] which represents a combination of LDOT and upper order-to-disorder transition (UDOT) behavior in individual specimens. This behavior is thought to arise from a delicate balance between enthalpic interactions and contributions from free volume effects and noncombinatorial entropy. Such effects also may be important in other weakly interacting polymer systems, including polyolefins.

Our group has studied the mixing behavior of various combinations of saturated hydrocarbon polymers for nearly two decades. PCHE-based block copolymers are especially attractive, both from the perspective of industrial application as mechanically stiff yet tough materials[4,7,37] and as model substrates for

* To whom correspondence should be addressed: e-mail bates@cems.umn.edu.

10.1021/ma071132g CCC: $37.00
Published on Web 08/11/2007

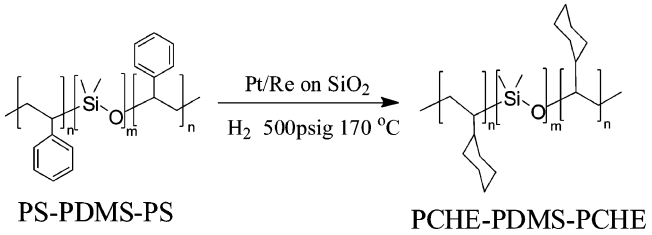

Figure 1. Reaction schematic of hydrogenation of PS−PDMS−PS triblock copolymer to make PCHE−PDMS−PCHE triblock copolymer.

exploring basic polymer blend thermodynamics.[11,24,25,38] In this paper, we report a block copolymer composed of PCHE and PDMS blocks. PDMS has many interesting properties, such as low surface tension, low glass transition temperature, and biocompatibility. Adding PCHE can impart stiffness and thermal stability, thereby producing a more robust material with a potentially wider range of applications. We demonstrate a method to produce PCHE−PDMS−PCHE triblock copolymers by the catalytic hydrogenation of PS−PDMS−PS precursor block copolymers using a Pt/Re−SiO_2 catalyst provided by the Dow Chemical Co. Figure 1 illustrates the hydrogenation reaction that forms the basis for this report. We also have investigated the thermodynamic properties of the saturated block copolymers using dynamic mechanical spectroscopy (DMS) and small-angle X-ray scattering (SAXS) techniques. In addition, we discuss the mixing thermodynamics of PCHE and PDMS in the context of solubility parameters and the concept of conformational asymmetry. To the best of our knowledge, this is the first report of the successful preparation of block copolymers containing PCHE and PDMS.

Experimental Section

PS−PDMS−PS Synthesis. PS−PDMS−PS triblock copolymers, precursors to PCHE−PDMS−PCHE triblock copolymers, were synthesized by sequential anionic polymerization of styrene and hexamethylcyclotrisiloxane (D_3) monomers, followed by chain coupling with dichlorodimethylsilane.

Styrene monomer (Aldrich) was degassed by three freeze−pump−thaw cycles followed by twice stirring with dibutylmagnesium (1 h each) before finally distilling into a flamed buret. D_3 monomer (Aldrich) was degassed in a similar fashion followed by stirring over calcium hydride (4 h) and dibutylmagnesium (1 h) and final distillation into a flamed buret.[39] D_3 monomer was held at 90 °C in a liquid state during these operations using a silicon oil bath. Cyclohexane was purified by sequential passage through columns of activated alumina and Q5 catalyst (Engelhard). Tetrahydrofuran (THF) was purified by passing through two activated alumina columns.[40] Solvents were collected into sealed flasks under anhydrous conditions using Schlenk techniques.

Anionic polymerization of the PS−PDMS−PS triblock copolymers was conducted under an argon atmosphere in a Pyrex reactor fitted with Teflon ferrules and screw caps. A more detailed description of the experimental setup was presented in a previous report.[41] Styrene was initiated in cyclohexane at 40 °C using *sec*-butyllithium; the presence of polystyryl anions was indicated by a deep orange color. Polymerization proceeded for 6 h, after which a small aliquot was extracted from the reactor for later analysis. Subsequently, D_3 monomer was added to the reactor, and the contents were stirred for 12 h at 25 °C. Prior work suggests complete crossover to siloxyl anions under these conditions.[39] However, polymerization of D_3 is very slow in nonpolar solvents such as cyclohexane, and therefore, sufficient THF was added to make a 50:50 mixture with the cyclohexane. The solution became colorless immediately after the addition of THF, indicating the onset of D_3 polymerization. This cyclic monomer was polymerized for 1.5 h (∼33% conversion), and the growing polymer chains were coupled by adding a stoichiometric amount of dichlorodimethylsilane. D_3 monomer was not polymerized to high conversions to prevent side reactions and oligomer formation, which become competitive with the polymerization at higher conversions. The polymers were recovered by solvent evaporation, redissolution in THF, and precipitation into a 50/50 mixture of methanol/isopropanol before finally drying to constant mass at 80 °C under vacuum (∼10^{-1} Torr). Polystyrene homopolymer (ca. 3% of the total mass) was detected in all the triblock copolymers due to some termination of the first block. This was removed by titrating a 2% polymer solution in dioxane with a 50:50 mixture of methanol/water at room temperature until it turned cloudy.[42,43] The block copolymer formed a floating mass, while the homopolymer remained dissolved in the solution.

Table 1. Notations and Chemical Structure for Various Blocks

Polymer	Chemical Structure	ρ^a (g/cm^3)	b (Å)^b
PCHE		0.92	4.60
PE		0.78	8.35
PEE		0.81	5.39
PEP	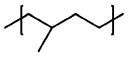	0.79	6.84
PDMS		0.89	5.39

[a] Mass density at 140 °C.[45] [b] Statistical segment length with respect to 118 Å^3 monomer reference volume.[45]

Catalytic Hydrogenation. PCHE−PDMS−PCHE triblock copolymers were prepared by catalytic hydrogenation of the PS blocks in PS−PDMS−PS triblock copolymers. These reactions were conducted in a stainless steel pressure vessel described elsewhere.[44] The polymer solution (5 g of polymer in 500 mL of cyclohexane) and the catalyst (1 g) were poured into the reaction vessel, which was then sealed and purged three times with nitrogen. Reactor contents were subsequently pressurized to 500 psi with hydrogen gas and heated to 170 °C with intense stirring. The reaction was carried out for 5 h, after which heating and stirring were stopped and the reactor contents were cooled to room temperature. The catalyst was removed by filtering the polymer solution through a 0.22 μm Durapore membrane filter (Millipore), and the polymer was recovered by solvent evaporation and drying to constant mass at 80 °C under vacuum (10^{-1} Torr).

Molecular Characterization. The compositions and the extent of hydrogenation of the block copolymers were determined from ^{1}H NMR spectra collected with a 300 MHz Varian instrument using deuterated chloroform as the solvent. PS and PCHE volume fractions were calculated using the reported homopolymer densities at 140 °C (Table 1).[45]

Number-average molecular weights (M_n) of all specimens were calculated using the M_n value for the PS block of precursor material (extracted during the synthesis), measured using a PS-calibrated SEC trace. Combining the composition (NMR) and M_n for PS block yielded the overall M_n. SEC was also used to determine the polydispersity of the block copolymers before and after the hydrogenation to establish whether the hydrogenation process led to any broadening of the molecular weight distribution.

Small-Angle X-ray Scattering (SAXS). SAXS experiments were carried out to characterize the morphology and the order−disorder transition temperature (T_{ODT}'s) of the saturated block copolymers. Experiments were conducted on a home-built system[46] using Cu Kα radiation and a Siemens area detector located at a distance of 230 cm from the sample. The morphology was deduced from the ratio of primary peak position to higher order peak

Table 2. Polymer Characterization Results

sample	$10^3 M_n$[a] (g/mol)	f[b]	PDI[c]	N[d]	T_{ODT} (°C)[e]
CDC-4	15.2	0.41	1.09	235	103
CDC-5	17.1	0.45	1.07	265	183
CDC-1	31.8	0.41	1.09	494	>250

[a] As calculated from mass fraction and M_n of precursor PS block. [b] Volume fraction of PCHE calculated from NMR using densities reported in Table 1. [c] From SEC based on polystyrene standards. [d] Degree of polymerization based on reference volume of 118 Å^3. [e] As determined by the discontinuity in elastic modulus during isochronal temperature ramp.

positions, and the T_{ODT} was identified by the onset of primary peak broadening and a sharp decrease in the intensity of the SAXS pattern. To deduce the morphology, samples were shear-aligned[47] using a reciprocating shear device[48] and then exposed to X-rays for 30 min at 25 °C while recording the scattering patterns. Measurements for T_{ODT} identification were performed by systematically heating the samples in small temperature steps (3−5 °C) and holding the sample at each temperature for 8 min before exposing it to the X-ray beam for another 8 min.

Transmission Electron Microscopy (TEM). TEM was employed for direct visualization of morphology of the block copolymers using a JEOL 1210 microscope operated at an accelerating voltage of 120 kV. Shear-aligned samples were cryomicrotomed to obtain 50−80 nm thick slices using a diamond knife operated between −130 and −145 °C on a Reichert Ultracut S ultramicrotome.[46] No staining was necessary, as the silicon in the PDMS block provides adequate contrast for imaging.[42]

Dynamical Mechanical Spectroscopy (DMS). DMS provided an independent measure of the T_{ODT}'s. Measurements were conducted on a Rheometrics Scientific ARES strain-controlled rheometer fitted with 25 mm parallel plates. All samples were compression-molded into 25 mm × 1 mm disks by holding them at 1000 psi and 150 °C for 10 min. Sample temperature in the rheometer was controlled (±1 °C) with a thermally regulated nitrogen gas purge. Elastic (G') and loss (G'') moduli were recorded at a constant frequency over a selected range of temperatures while heating or cooling the samples. Disordering (ordering) of the block copolymer materials was identified by a discontinuous decrease (increase) in G' and G''.[49]

Results and Analysis

Three PS−PDMS−PS triblock copolymers containing 41−45 vol % of polystyrene were prepared and hydrogenated to produce PCHE−PDMS−PCHE triblock copolymers. The samples were designed specifically to have accessible ODT temperatures. The molecular characterization data for all three polymers appear in Table 2.

Representative ^{1}H NMR spectra for the PCHE−PDMS−PCHE triblock copolymer (CDC-5), and the unsaturated precursor PS−PDMS−PS, are shown in Figure 2. Complete hydrogenation of polystyrene (>99%) is marked by the disappearance of specific resonances associated with the aromatic protons (6.2−7.2 ppm) in the ^{1}H NMR spectra of the saturated product (Figure 2B).

SEC traces are shown in Figure 3. Trace b for the PS−PDMS−PS triblock shows the presence of a small amount of polystyrene homopolymer impurity (around an elution time of 24 min), which was removed using the precipitation technique described in the previous section (trace c). Hydrogenation yielded the saturated PCHE−PDMS−PCHE triblock copolymer depicted by the trace d. Saturation did not noticeably affect the polydispersity of this sample, although a small amount (ca. 1%) of low molecular weight polymer is barely resolved in the SEC trace of the hydrogenated triblock (trace d, around an elution time of 24 min), perhaps indicating some (PDMS) chain degradation during the hydrogenation reaction. All saturated polymers contained a similar amount of this impurity, with a

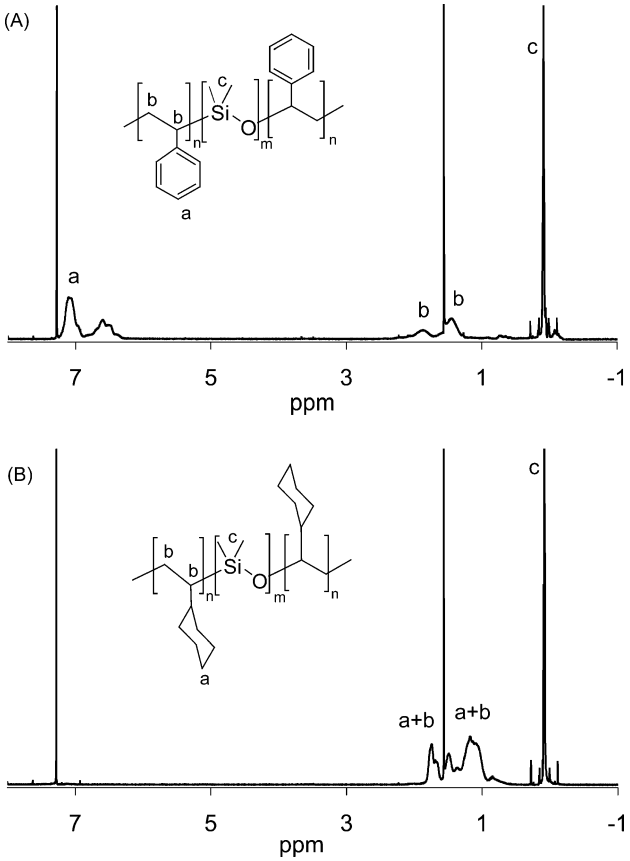

Figure 2. ^{1}H NMR spectra of (A) PS−PDMS−PS triblock copolymer and its hydrogenated form (B) PCHE−PDMS−PCHE triblock copolymer. The aromatic resonances (6−7.5 ppm) of the PS−PDMS−PS triblock copolymer are converted into the cyclic resonances (1−2 ppm) after hydrogenation. The sharp peaks at 7.3 and 1.5 ppm are due to residual chloroform and water in the solvent.

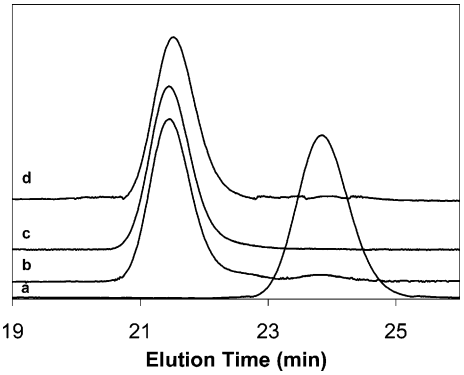

Figure 3. Size exclusion chromatograph of (a) polystyrene aliquot, (b) PS−PDMS−PS triblock copolymer obtained after polymerization, (c) PS−PDMS−PS triblock purified by precipitation using dioxane−methanol/water mixture to remove polystyrene homopolymer impurity, and (d) PCHE−PDMS−PCHE triblock obtained after catalytic hydrogenation. The molecular weight distribution is unaffected by hydrogenation indicated by comparable polydispersity indices. Curves have been shifted vertically for clarity.

M_n value close to that of precursor PS block, presumably created by the spurious scission of PDMS. We believe this minor level of degradation will not significantly impact the properties of the saturated triblock copolymers.

The morphology of the saturated polymers was characterized using SAXS and TEM. 2-D SAXS data obtained at 25 °C were integrated azimuthally to yield the intensity (I) as a function of scattering wavevector $q = (4\pi/\lambda)\sin(\theta/2)$, as shown in Figure 4. Two reflections are clearly evident in the data obtained from

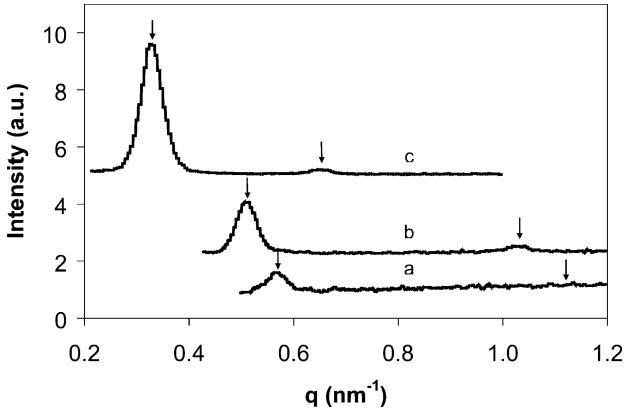

Figure 4. 1-D SAXS profiles obtained from shear aligned samples at 25 °C: (a) CDC-4, (b) CDC-5, and (c) CDC-1. The vertical arrows denote peak locations expected for a lamellar microstructure. Curves have been shifted vertically for clarity.

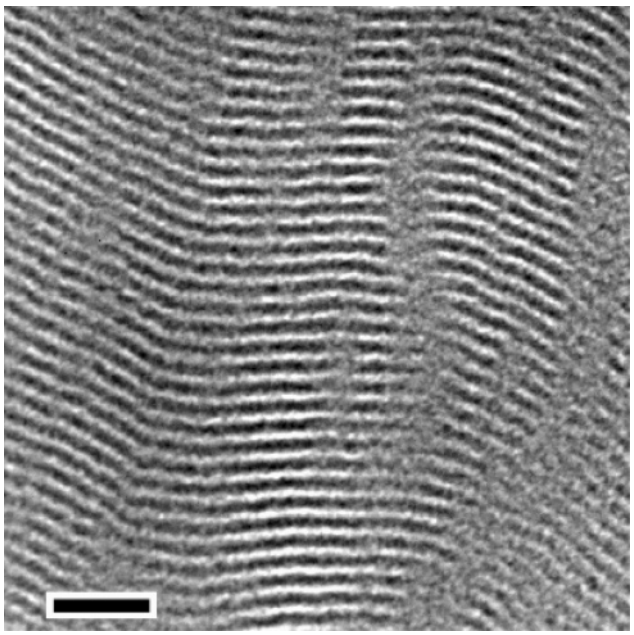

Figure 5. TEM image of CDC-5 indicating a lamellar morphology of the block copolymer. The lamellar domains were aligned by applying reciprocating shear,[35] followed by cryo-microtomy to obtain thin slices of polymer for imaging. Dark and light regions correspond to PDMS and PS domains. The scale bar represents 50 nm.

samples CDC-1 and CDC-5 at relative q values 1:2, consistent with a lamellar morphology. For CDC-4, only one peak is evident. Also, a reduced overall scattering intensity was obtained with this lower molecular weight specimen. All three samples were found to contain a lamellar morphology by direct visualization of cryo-microtomed polymer slices by TEM. Figure 5 shows a representative TEM image of the CDC-5 sample.

T_{ODT} values were determined for the saturated polymers by SAXS as described earlier. Figure 6 shows 1-D SAXS profiles for the three samples at various temperatures. A sharp decrease in the scattering intensity is visible around a temperature of 103 °C for CDC-4 (Figure 6a) and 181 °C for CDC-5 (Figure 6b), indicating the ODT. CDC-1 remained ordered up to 200 °C (Figure 6c), which was the highest temperature accessed in this work. All samples were subjected to repeated cycles of heating and cooling during SAXS testing, resulting in reproducible values of T_{ODT} for CDC-4 and CDC-5.

ODT temperatures were independently determined by DMS. CDC-1 was tested at a frequency of 1 rad/s between 100 and 250 °C with a heating/cooling rate of 1 °C/min. CDC-4 was tested at 0.1 rad/s between 95 and 114 °C with a heating/cooling rate of 0.2 °C/min, and CDC-5 was tested at 1 rad/s between 150 and 200 °C with a heating/cooling rate of 2 °C/min. A strain amplitude of 1% was employed for all three samples. Figure 7 shows the elastic modulus (G') vs temperature for CDC-4 and CDC-5 during heating and the cooling cycles. ODTs are identified by the precipitous drop in elastic moduli (G') during the heating cycle.[49] Using this technique, T_{ODT} was established to be 103 ± 1 °C for CDC-4 and 183 ± 1 °C for CDC-5, as indicated in Figure 7. These values are within experimental uncertainty of those obtained by the SAXS experiments. Samples were subjected to multiple heating and cooling cycles, verifying the reproducibility of the ODT temperature measurements. CDC-1 did not show any discontinuous decrease in G' up to a temperature of 250 °C (data not shown), indicating an ordered microstructure. Higher temperatures (>250 °C) were not explored in order to avoid degradation of the polymer.

Thermodynamic Behavior

Polymer−polymer phase behavior can be deceptively complex. Local (segment scale) interactions are governed by both enthalpic and entropic factors. Polyolefins present a particularly challenging set of materials since the enthalpic driving force for demixing is quite weak, thus amplifying nonideal contributions to the overall mixing free energy. A widely accepted approach to treating polymer mixtures is to employ a mean-field theory, in which the phase behavior of block copolymers is assumed to be governed by a simple binary segment−segment interaction parameter, captured by the Flory−Huggins interaction parameter χ, which is often written in the form

$$\chi = \frac{A}{T} + B \tag{1}$$

Equation 1 lumps the enthalpy of mixing and various excess free energy contributions into the parameter A and B, respectively.[38] Sometimes, A and B in eq 1 are assumed to be composition or molecular weight dependent in order to accommodate specific interactions like hydrogen bonding and various equation-of-state effects such as volume changes on mixing, thermal expansion differences, and component compressibilities.[50,51] However, in this report we focus on determining $\chi(T)$ by considering a single composition and pressure and neglecting other dependencies.

To this end, $\chi(T)$ can be extracted experimentally from a set of block copolymers by applying mean-field theory, either with or without a fluctuation correction.[20] For diblock copolymers, Maurer et al.[13] have shown that combining the mean-field result[16] $(\chi N)_{ODT} = 10.5$ for $f = 0.5$ with the ODT measurements gives the closest approximation to the $\chi(T)$ expression obtained from homopolymer blends. (Here N is the overall degree of polymerization, and f is the volume fraction of the first block.) Matsen et al.[14] and Mayes et al.[12] have extended mean-field theory calculations from diblock copolymers to symmetric ABA triblock copolymers, yielding

$$\chi(T_{ODT}) = 19/N \quad (\text{for } f = 0.45) \tag{2a}$$

and

$$\chi(T_{ODT}) = 20/N \quad (\text{for } f = 0.41) \tag{2b}$$

where f is the total volume fraction of block A and N is the overall degree of polymerization normalized to a chosen reference volume. For our analysis, we have chosen a reference

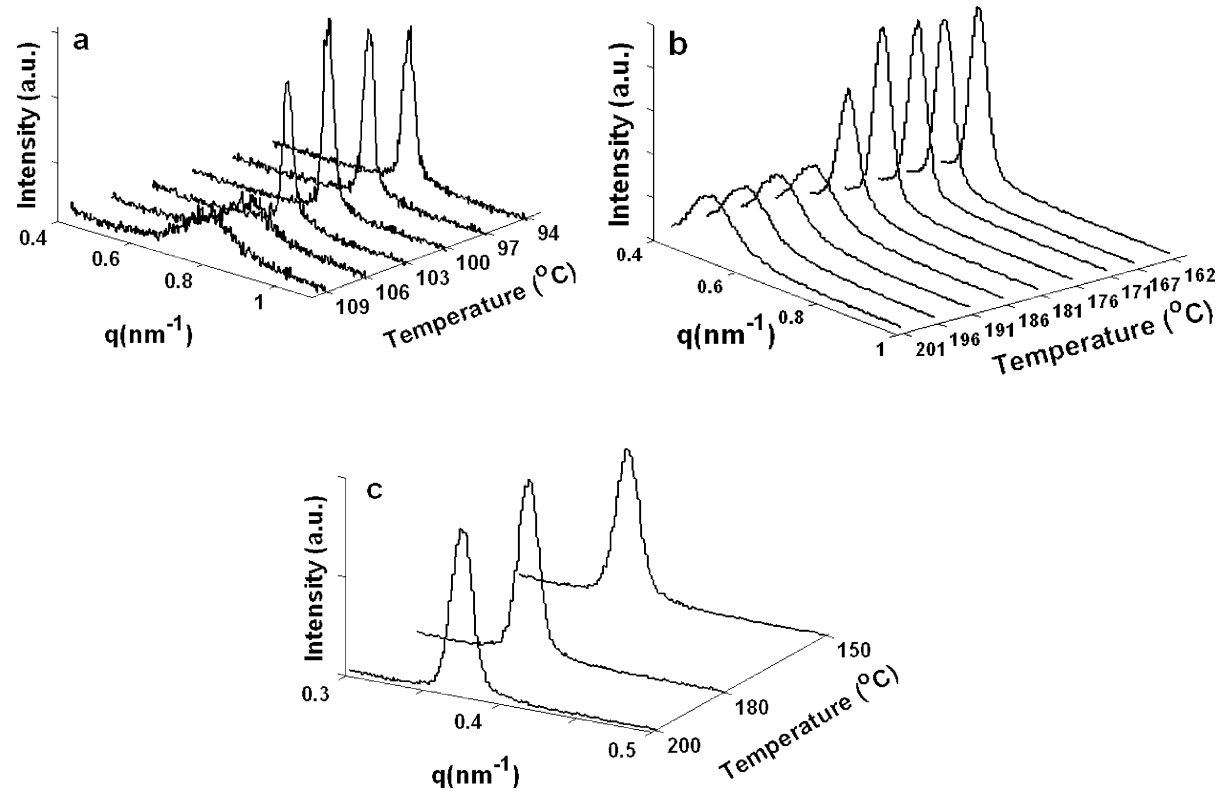

Figure 6. 1-D SAXS profiles at various temperatures for (a) CDC-4, (b) CDC-5, and (c) CDC-1. A sharp decrease in the scattering intensity and broadening of peak marks the onset of ODT.

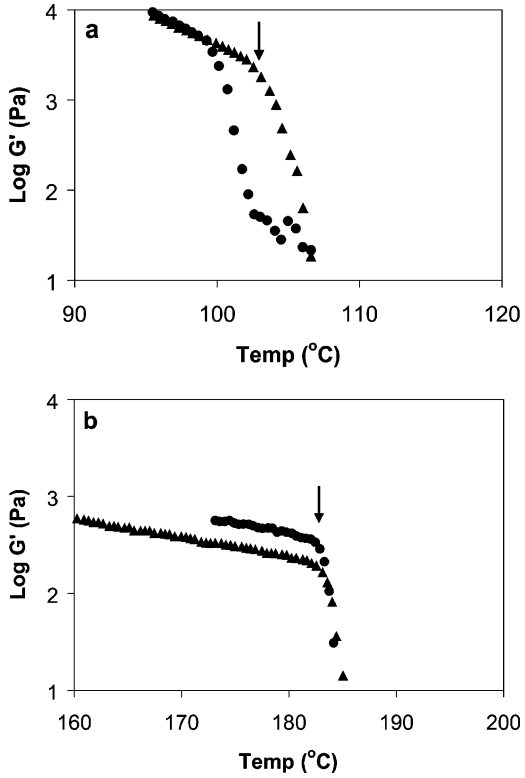

Figure 7. Dynamic elastic modulus (G') during the heating (▲) and cooling (●) cycles of an isochronal temperature test for (a) CDC-4 and (b) CDC-5. For CDC-4, the heating/cooling rate was 0.2 °C/min, and the frequency was 0.1 rad/s. For CDC-5, the heating/cooling rate was 2 °C/min and the frequency was 1 rad/s. The ODT is marked by a sharp decrease in G', as indicated by the arrows in the figures.

volume of 71.1 cm^3/mol (118 $Å^3$ per repeat unit), which is approximately the molar volume of most four-carbon polyolefin segments. This choice of reference volume is consistent with previous reports[24,38] and facilitates comparison of χ parameters between different pairs of polyolefins. Parameters A and B are obtained by least-square fit to the χ vs T data obtained for samples with different values of N. It should be noted that we are neglecting fluctuation effects in this approach, so there may be a slight error in the χ values we report; nevertheless, the qualitative features of this analysis should still be useful.

On the basis of T_{ODT} and N (Table 2) for samples CDC-4 and CDC-5, we determined the expression for $\chi(T)$ between PCHE and PDMS to be

$$\chi = \frac{28.1}{T} + 1.0 \times 10^{-2} \tag{3}$$

Here we note that the A and B values extracted from χ vs T data are sensitive to uncertainties in molecular weights of the samples. An error of about ±5% in molecular weight (associated with uncertainties in SEC and NMR measurements) can change the above expression from $\chi = 37.8/T - 1.1 \times 10^{-2}$ to $\chi = 19.8/T + 31.9 \times 10^{-2}$, although the overall χ values are still within a range of ±5%. Thus, it is safer to draw quantitative conclusions regarding the magnitude of the χ values. (Of course, establishing that χ is linear in T^{-1}as indicated by eq 3 requires additional T_{ODT} measurments and hence additional CDC specimens with varying molecular weight.)

For saturated hydrocarbons, χ is often estimated using the difference in solubility parameters based on the Hildebrand equation[52]

$$\chi_{AB} = \frac{v}{k_B T}(\delta_A - \delta_B)^2 \tag{4}$$

where v is the reference volume (118 $Å^3$) and δ_A and δ_B represent the pure component solubility parameters for the constituent polymers. This approach neglects the excess free energy terms (accounted for by the parameter B in eq 1) and

Table 3. Fitted Parameters in $\chi = A/T + B$ and Solubility Parameter Differences $|\Delta\delta|$ Calculated from Eq 4

polymer pair	A (K)	$B \times 10^3$	$\chi \times 10^3$ (456 K)	$\lvert\Delta\delta\rvert$ $(\text{MPa})^{1/2}$	ref
PE−PDMS	90.7	−94.6	104	2.36	38
PEP−PDMS	41.4	−23.7	67.1	1.89	38
PEE−PDMS	25.4	−20.9	34.8	1.36	38
PCHE−PE	29.4	−17.4	47.1	1.58	24
PCHE−PEE	11.2	−8.70	15.9	0.92	24
PCHE−PEP	15.7	−3.60	30.8	1.28	24
PE−PEP	8.87	−16.0	3.47	0.43	38
PEP−PEE	3.66	1.37	9.40	0.71	38
PE−PEE	12.1	−4.90	21.6	1.07	38
PCHE−PDMS	28.1	10.0	71.6	1.95	this work

considers only dispersive interactions. Polyolefins are often assumed to be the most likely candidates to conform to eq 4, as they are governed primarily by dispersive van der Waals forces. Graessley and co-workers[8,17,18,53−55] have shown that in 75% of the polyolefin blends they studied experimentally measured χ values lead to a self-consistent set of δ_i's. Cochran and Bates[24] extended this approach to diblock copolymers containing PCHE and other polyolefins and were able to rationalize the χ values with a self-consistent set of δ_i's. Almdal et al.[38] have applied this approach to block copolymers containing various polyolefins with PDMS and also were able to correlate the χ values with a set of self-consistent δ_i's. This work adds PCHE−PDMS to this matrix of data. All relevant parameters are listed in Table 3. χ values for all polymer pairs are compared at 456 K. This temperature was chosen on the basis of the experimentally obtained T_{ODT} for sample CDC-5. However, a different choice of the temperature over the normally accessed temperature range of 100−200 °C does not affect our general conclusions.

Discussion

Various approaches have been utilized in the past to rationalize the thermodynamic behavior of polyolefin block copolymers and blends of polyolefin homopolymers. As mentioned in the previous section, a self-consistent set of solubility parameters explains the phase behavior of a host of polymer blends but fails for about 25% of the blends investigated by Graessley and co-workers.[8,17,18,53−55] Another approach based on segment length mismatch, suggested by Bates et al.,[25] provides a rationale for the observed phase behavior in many polymer systems but fails to make the quantitative predictions. Several more sophisticated theories have been put forward, which incorporate factors such as polymer compressibility,[10,21,56,57] conformational asymmetry,[22,23,26,58] and segment architecture,[21,59−62] parameters not accounted by traditional Flory−Huggins theory. Fredrickson and co-workers[26,58] have suggested an excess entropy contribution to free energy arising from the structural asymmetry of polymer chains. Dudowicz and Freed[21,59] have developed a lattice cluster theory for compressible diblock copolymers, which considers polymer segment architectures in great detail. Schweizer and co-workers[10,22,23] have developed an off-lattice method that relies on the polymer reference interactive site model (PRISM), which addresses local and nonlocal aspects of polymer−polymer mixing. These theories attempt to address the thermodynamic behavior of actual polymer blends and block copolymer systems. Figure 8 plots the $\chi(T)$ data extracted from the PCHE−PDMS−PCHE triblock copolymer (eq 3) along with other olefinic block copolymers reported in previous publications.[11,24,38,49] A and B parameters and estimated solubility parameter differences $|\Delta\delta|$ are listed in Table 3.

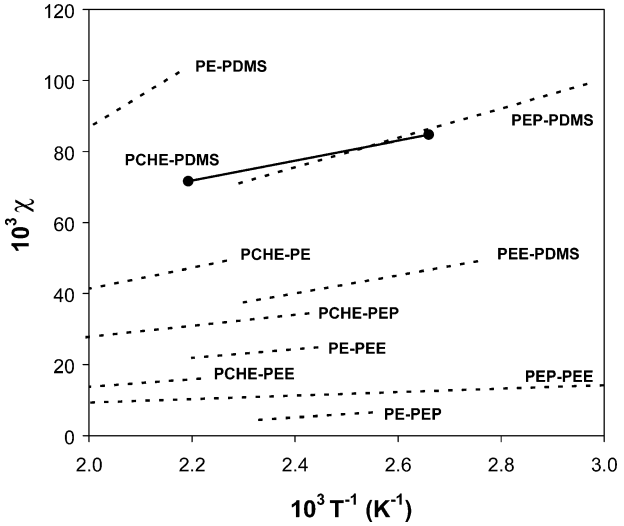

Figure 8. Temperature dependence of χ_{AB} (based on T_{ODT}) for various olefinic block copolymers. Data points (●) correspond to PCHE−PDMS−PCHE triblock copolymers (see Table 2), and solid line is to evaluate parameters A and B of eq 1. Dashed lines are correlations for various block copolymers taken from previously published data.[11,24,38]

Graessley and co-workers have established the following order of solubility parameters based on deuterium-labeling experiments[54,55]

$$\delta_{PEE} < \delta_{PEP} < \delta_{PE} \quad \text{(see Table 1 for block notations)}$$

Cochran and Bates[24] added PCHE to this sequence (see Table 3). Self-consistency of the solubility parameters suggests the following order:

$$\delta_{PCHE} < \delta_{PEE} < \delta_{PEP} < \delta_{PE}$$

Almdal et al.[38] obtained the following order for various PDMS−polyolefin block copolymers:

$$\Delta\delta_{PEE-PDMS} < \Delta\delta_{PEP-PDMS} < \Delta\delta_{PE-PDMS}$$

Self-consistency among these three sets of results necessitates the following order:

$$\delta_{PDMS} < \delta_{PCHE} < \delta_{PEE} < \delta_{PEP} < \delta_{PE}$$

In terms of the solubility parameter differences, this implies that $\Delta\delta_{PCHE-PDMS}$ should be smaller than $\Delta\delta_{PEP-PDMS}$ and $\Delta\delta_{PEE-PDMS}$. However, the solubility parameter difference calculated from the ODT data for PCHE−PDMS−PCHE triblock copolymer, listed in Table 3, leads to $\Delta\delta_{PCHE-PDMS} \approx \Delta\delta_{PEP-PDMS}$ and $\Delta\delta_{PCHE-PDMS} > \Delta\delta_{PEE-PDMS}$. Thus, PCHE−PDMS challenges the self-consistency between the solubility parameters reported previously.

Bates et al.[25] have suggested an alternative approach to explain the experimentally determined χ values in polyolefin block copolymers. They argue that the differences in statistical segment lengths of the constituent blocks in polyolefin block copolymers are strongly correlated with the measured χ values. Holding all other factors constant, χ is expected to increase with increasing mismatch of the statistical segment lengths of the constituent blocks. This change in χ is attributed to entropic penalties associated with the conformational adjustments required to mix chains of different statistical segment lengths. This effect becomes particularly important with polyolefin mixtures, since the enthalpy of mixing is relatively small. Hence, the effects of excess entropy can play a dominant role in

Table 4. Various Parameters for PDMS Containing Polyolefin Block Copolymers

polymer pair	$\Delta b/\bar{b}$[a]	$\Sigma\beta^2$[b] ($Å^{-1}$)	ϵ[c]	$[(1-\epsilon)/(f+(1-f)\epsilon)]^2$[d]	γ[e]	$\chi \times 10^3$ (at 456 K)	$\chi_\epsilon \times 10^3$[f]	Λ_b^{-1}[g] (Å)
PEE−PDMS	≈0	0.082	1.00	≈0	1.00	34.8	0	
PCHE−PDMS	0.16	0.071	0.73	0.10	0.85	71.6	36.8	1.10
PEP−PDMS	0.24	0.107	1.61	0.22	1.27	67.1	32.3	1.50
PE−PDMS	0.43	0.140	2.40	0.68	1.55	104	69.2	1.69

[a] Segment length mismatch parameter defined in eq 5.[25] [b] The *z*-effect parameter defined in eq 6.[38] [c] Conformational asymmetry parameter calculated from eq 9[26] using statistical segment lengths listed in Table 1. [d] Asymmetry factor in eq 8. [e] Asymmetry parameter in eq 10.[22,23] [f] Excess entropy contributions to χ parameter calculated by assuming a zero excess entropy contribution for PEE−PDMS pair. [g] Cutoff length that separates local and nonlocal conformational regimes (eq 8).[26,58]

determining the phase behavior of these systems. Scaling of the χ parameter with segment length mismatch has been noted for PDMS containing polyolefin block copolymers[38] and many other polymer systems,[18,19] and theoretical explanations have also been provided for the same.[26,58]

Table 4 lists the χ parameter values for various PDMS containing polyolefin block copolymers studied in our group including this work. Segment length mismatch is defined by the ratio $\Delta b/\bar{b}$, as suggested by Bates et al.:[25]

$$\frac{\Delta b}{\bar{b}} = \frac{b_A - b_B}{f b_A + (1-f) b_B} \tag{5}$$

where b represents statistical segment length and f is the volume fraction of block A. The segment length mismatch argument anticipates a higher χ value for PEP−PDMS than for PCHE−PDMS, which is inconsistent with our experimental observation (compare $\Delta b/\bar{b}$ and χ values in Table 4).

A third argument to explain the experimentally observed χ parameter values, given by Almdal et al.,[38] is based on the so-called "z effect", which is associated with the parameter $\Sigma\beta^2$:

$$\sum \beta^2 = \beta_A{}^2 + \beta_B{}^2 \tag{6}$$

with

$$\beta^2 = \frac{b^2}{6v} \tag{7}$$

where v is the reference volume (118 $Å^3$). The authors suggested that polymers with larger β^2 value offer more contacts with neighboring chains, leading to a higher effective chain−chain coordination number, *z*. Higher *z*, in turn, enhances the total enthalpic contribution to the χ parameter. On the basis of the values of the parameter $\Sigma\beta^2$ for polyolefin−PDMS block copolymers (listed in Table 4), the *z* effect argument anticipates that both $\chi_{PEP-PDMS}$ and $\chi_{PEE-PDMS}$ will be greater than $\chi_{PCHE-PDMS}$, while experimentally we observe that $\chi_{PEP-PDMS} \approx \chi_{PCHE-PDMS}$ and $\chi_{PEE-PDMS}$ is about half the value of $\chi_{PCHE-PDMS}$.

The three factors introduced in the previous paragraphs (solubility parameter, excess entropy, and excess enthalpy) can add constructively or destructively, leading to the overall χ parameter. However, no combination of these factors can simultaneously explain the experimentally recorded behavior of PEP−PDMS and PCHE−PDMS ($\chi_{PEP-PDMS} \approx \chi_{PCHE-PDMS}$). This indicates that the relatively simple approaches to explaining polyolefin, and other nonpolar polymer, phase behavior fail to capture all the essential molecular factors that govern mixing and demixing.

Fredrickson et al.[26,58] have developed a theory for athermal, conformationally asymmetric, polymer alloys using incompressible field theoretic methods. They argued that the lack of conformational symmetry in athermal block copolymers and polymer blends produces excess entropy of mixing which results in an additional contribution to the χ parameter. This excess contribution χ_ϵ to overall effective χ parameter is given by the equation

$$\chi_\epsilon = \frac{\Lambda_b{}^3 v}{24\pi^2}\left[\frac{1-\epsilon}{f+(1-f)\epsilon}\right]^2 \tag{8}$$

where $\Lambda_b{}^{-1} > b$ is a cutoff length that separates the local and nonlocal conformational regimes and ϵ is the conformational asymmetry parameter given by

$$\epsilon = \frac{\beta_A{}^2}{\beta_B{}^2} \tag{9}$$

Block copolymers of PDMS with various polyolefins cannot be treated as strictly athermal since the enthalpic interactions between PDMS and polyolefin segments are likely to differ from PDMS−PDMS and polyolefin−polyolefin segment interactions. However, within the context of this theory, the enthalpic interactions should not vary from one polyolefin−PDMS block copolymer to another. Thus, it would be reasonable to expect that the differences in χ parameter values observed for various polyolefin−PDMS block copolymers are due to entropically based conformational asymmetry effects between the constituent blocks.

The form of eq 8 requires the excess entropy contributions to vanish for conformationally matched polymers ($\epsilon = 1$) and to be positive for conformationally mismatched pairs ($\epsilon < 1$ or $\epsilon > 1$). Thus, for the PEE−PDMS pair, $\chi_\epsilon = 0$, and χ_ϵ for the other pairs can be estimated by subtracting $\chi_{PEE-PDMS}$ from experimentally obtained χ values for other block copolymers. Following this procedure, we obtain positive χ_ϵ values for the conformationally mismatched polymers listed in Table 4. Relatively good agreement with experimental data can be obtained by adjusting the cutoff length Λ_b^{-1} in eq 8. Also, one would expect the cutoff length to increase from PCHE−PDMS to PE−PDMS on the basis of increasing statistical segment length in this direction (and hence influence of local liquid structure on a larger scale). This is indeed the trend we obtain (see Λ_b^{-1} values in Table 4). However, the values of the cutoff lengths obtained are unreasonably low (i.e., $\Lambda_b^{-1} < b$), which represents a limitation of this theory and suggests that certain important factors are not accounted for. Also, it is somewhat unclear how to assign a precise value to cutoff length once we know the constituent blocks, rather than treating it as a fitting parameter.

Dudowicz and Freed have constructed a comprehensive lattice cluster theory (LCT) for polymer blends[62] and block copolymers[21,59] which accounts for detailed variations in local chain structure. This theory has provided a rationale for understanding various extensions of Flory−Huggins theory (for e.g., presence of an entropic contribution to χ, concentration dependence of χ, equation-of-state effects, etc.). The authors have also addressed the issue of conformational asymmetry in some detail

for polyolefin blends. However, the theory is very system specific and does not anticipate trends for block copolymer thermodynamics. A comparison with our experimental data would require a detailed evaluation of this theory for polyolefin−PDMS block copolymers, incorporating finer details of monomer structure and interaction parameters, which is beyond the scope of this paper.

A comprehensive theoretical treatment of polymer blend thermodynamics based on the polymer reference interactive site model (PRISM) has been developed by Schweizer and coworkers.[10,22,23,56,57] This approach accounts for local chain packing and polymer architecture, volume change upon mixing, thermally induced changes in chain dimensions, and various other non-Flory−Huggins effects that are neglected in the mean-field approach. This theory uses off-lattice methods, which allows making general predictions on polymer thermodynamics based on coarse-grained descriptions of polymer chains. The authors have made general predictions regarding the influence of conformational asymmetry and local packing on the thermodynamic properties of block copolymers.[22,23] They argue that mixtures of polyolefins cannot be treated as athermal despite the fact that the actual mean attractive interactions may nearly cancel. Microphase separation in these block copolymers can be traced to local enthalpic interactions, convoluted with conformational asymmetry induced packing differences; excess entropy contributions are very small in comparison and do not play a major role. This treatment is in contrast with the incompressible field theoretical approach of Fredrickson et al.[26,58] discussed earlier, wherein a spatially nonlocal excess entropic contribution to the effective χ parameter was suggested to be responsible for the structure dependent phase instabilities, with energetic effects being treated as a small additive empirical correction.

David and Schweizer[22,23] have explicitly studied the consequences of varying the conformational asymmetry in polyolefin diblock copolymers, keeping one of the blocks the same, consistent with this work, where we have combined various polyolefins with PDMS. The authors identify the apparent spinodal temperature, $T_{s,app}$, as an indicator of the proximity to the true microphase separation transition occurring at T_{ODT}, for polymers with varying degrees of chain stiffness. Conformational symmetry was defined by the parameter γ, which was simply the ratio of statistical segment lengths:

$$\gamma = \frac{b_B}{b_A} \tag{10}$$

We point out here that actual values of various statistical segment lengths used by David and Schweizer[22] arise from the mapping of real branched polymers to unbranched effective homopolymer chains, which will be different than those described in our work based on a common reference volume (Table 1). However, qualitative comparisons can still be made between their model predictions and our experimental data. The γ values for various polyolefin−PDMS block copolymers are listed in Table 4. The PRISM calculations predict that a deviation from conformational symmetry ($\gamma = 1$) increases $T_{s,app}$, consistent with the trend in the χ parameter observed in the polyolefin−PDMS block copolymers. Also, the model predicts that block copolymers with $\gamma = 0.85$ and $\gamma = 1.25$ will have approximately equal value of $T_{s,app}$. These γ values roughly correspond to PCHE−PDMS and PEP−PDMS, for which we observe approximately equal χ values. Thus, PRISM theory calculations with a coarse-grained polymer model for diblock copolymer melts seem to capture the trends in χ values obtained experimentally. A quantitative comparison will require mapping of the polyolefin−PDMS block copolymer chains onto a suitable model and taking into account the interaction asymmetry between polyolefin−polyolefin, PDMS−PDMS, and polyolefin−PDMS segments.

The results presented in this study indicate that the simplistic approaches based on the solubility parameter self-consistency and conformational asymmetry are not adequate to account for the mixing thermodynamics of PDMS with various polyolefins in the form of block copolymers. More sophisticated treatments such as the PRISM theory are more likely to capture the phase behavior of these polymers.

Summary

PS−PDMS−PS triblock copolymers were successfully hydrogenated to form PCHE−PDMS−PCHE triblock copolymers by heterogeneous catalytic hydrogenation. The hydrogenation process resulted in the complete hydrogenation of PS blocks with negligible chain scission. Triblock copolymers with PCHE volume fractions ranging from 0.41 to 0.45 segregate into a lamellar morphology. The thermodynamic properties of this new material were established using small-angle X-ray scattering and dynamical mechanical spectroscopy. PCHE and PDMS have a relatively strong segregation strength reflected in a rather high T_{ODT} of 180 °C for a relatively low molecular weight (M_n = 17 000 g/mol) PCHE−PDMS−PCHE triblock copolymer. In addition, the χ parameter value for the PCHE−PDMS polymer pair was found to be higher than PEE−PDMS and very close to that for PEP−PDMS, which cannot be rationalized by the solubility parameter approach or the simple arguments based on conformational asymmetry. A more elaborate theoretical treatment, such as PRISM theory, is needed to account for the nonideal mixing of these and other nonpolar polymers.

Acknowledgment. This work was made possible with the financial support from NSF (Grant NSF/CTS-0403574). The authors thank Dr. Alhad Phatak for help in hydrogenation and Qiang Lan for help with electron microscopy.

References and Notes

(1) Bates, F. S.; Fredrickson, G. H.; Hucul, D.; Hahn, S. F. *AIChE J.* **2001**, *47*, 762−765.
(2) Gehlsen, M. D.; Bates, F. S. *Macromolecules* **1993**, *26*, 4122−4127.
(3) Hucul, D. A.; Hahn, S. F. *Adv. Mater. (Weinheim, Germany)* **2000**, *12*, 1855−1858.
(4) Ryu, C. Y.; Ruokolainen, J.; Fredrickson, G. H.; Kramer, E. J.; Hahn, S. F. *Macromolecules* **2002**, *35*, 2157−2166.
(5) Patel, R. M.; Hahn, S. F.; Esneault, C.; Bensason, S. *Adv. Mater. (Weinheim, Germany)* **2000**, *12*, 1813−1817.
(6) Mori, Y.; Lim, L. S.; Bates, F. S. *Macromolecules* **2003**, *36*, 9879−9888.
(7) Hermel, T. J.; Hahn, S. F.; Chaffin, K. A.; Gerberich, W. W.; Bates, F. S. *Macromolecules* **2003**, *36*, 2190−2193.
(8) Balsara, N. P.; Fetters, L. J.; Hadjichristidis, N.; Lohse, D. J.; Han, C. C.; Graessley, W. W.; Krishnamoorti, R. *Macromolecules* **1992**, *25*, 6137−47.
(9) Zhao, J.; Majumdar, B.; Schulz, M. F.; Bates, F. S.; Almdal, K.; Mortensen, K.; Hajduk, D. A.; Gruner, S. M. *Macromolecules* **1996**, *29*, 1204−15.
(10) Schweizer, K. S.; Curro, J. G. *Macromolecules* **1988**, *21*, 3070−81.
(11) Rosedale, J. H.; Bates, F. S.; Almdal, K.; Mortensen, K.; Wignall, G. D. *Macromolecules* **1995**, *28*, 1429−1443.
(12) Mayes, A. M.; Olvera, de la Cruz, M. *J. Chem. Phys.* **1989**, *91*, 7228−35.
(13) Maurer, W. W.; Bates, F. S.; Lodge, T. P.; Almdal, K.; Mortensen, K.; Fredrickson, G. H. *J. Chem. Phys.* **1998**, *108*, 2989−3000.
(14) Matsen, M. W.; Thompson, R. B. *J. Chem. Phys.* **1999**, *111*, 7139−7146.
(15) Liu, A. J.; Fredrickson, G. H. *Macromolecules* **1992**, *25*, 5551−5553.
(16) Leibler, L. *Macromolecules* **1980**, *13*, 1602−1617.

(17) Krishnamoorti, R.; Graessley, W. W.; Fetters, L. J.; Garner, R. T.; Lohse, D. J. *Macromolecules* **1995**, *28*, 1252−1259.
(18) Graessley, W. W.; Krishnamoorti, R.; Reichart, G. C.; Balsara, N. P.; Fetters, L. J.; Lohse, D. J. *Macromolecules* **1995**, *28*, 1260−1270.
(19) Gehlsen, M. D.; Bates, F. S. *Macromolecules* **1994**, *27*, 3611−3618.
(20) Fredrickson, G. H.; Helfand, E. *J. Chem. Phys.* **1987**, *87*, 697−705.
(21) Dudowicz, J.; Freed, K. F. *J. Chem. Phys.* **1994**, *100*, 4653−4664.
(22) David, E. F.; Schweizer, K. S. *Macromolecules* **1997**, *30*, 5118−5132.
(23) David, E. F.; Schweizer, K. S. *Macromolecules* **1995**, *28*, 3980−3994.
(24) Cochran, E. W.; Bates, F. S. *Macromolecules* **2002**, *35*, 7368−7374.
(25) Bates, F. S.; Schulz, M. F.; Rosedale, J. H.; Almdal, K. *Macromolecules* **1992**, *25*, 5547−5550.
(26) Bates, F. S.; Fredrickson, G. H. *Macromolecules* **1994**, *27*, 1065−1067.
(27) Steinhoff, B.; Ruellmann, M.; Wenzel, M.; Junker, M.; Alig, I.; Oser, R.; Stuehn, B.; Meier, G.; Diat, O.; Boesecke, P.; Stanley, H. B. *Macromolecules* **1998**, *31*, 36−40.
(28) Schwahn, D.; Frielinghaus, H.; Mortensen, K.; Almdal, K. *Macromolecules* **2001**, *34*, 1694−1706.
(29) Frielinghaus, H.; Schwahn, D.; Mortensen, K.; Almdal, K.; Springer, T. *Macromolecules* **1996**, *29*, 3263−3271.
(30) Beiner, M.; Fytas, G.; Meier, G.; Kumar, S. K. *Phys. Rev. Lett.* **1998**, *81*, 594−597.
(31) Weidisch, R.; Stamm, M.; Schubert, D. W.; Arnold, M.; Budde, H.; Hoering, S. *Macromolecules* **1999**, *32*, 3405−3411.
(32) Russell, T. P.; Karis, T. E.; Gallot, Y.; Mayes, A. M. *Nature (London)* **1994**, *368*, 729−731.
(33) Hashimoto, T.; Hasegawa, H.; Hashimoto, T.; Katayama, H.; Kamigaito, M.; Sawamoto, M.; Imai, M. *Macromolecules* **1997**, *30*, 6819−6825.
(34) Ryu, D. Y.; Lee, D. H.; Jeong, U.; Yun, S.-H.; Park, S.; Kwon, K.; Sohn, B.-H.; Chang, T.; Kim, J. K.; Russell, T. P. *Macromolecules* **2004**, *37*, 3717−3724.
(35) Ryu, D. Y.; Jeong, U.; Kim, J. K.; Russell, T. P. *Nat. Mater.* **2002**, *1*, 114−117.
(36) Li, C.; Lee, D. H.; Kim, J. K.; Ryu, D. Y.; Russell, T. P. *Macromolecules* **2006**, *39*, 5926−5930.
(37) Phatak, A.; Lim, L. S.; Reaves, C. K.; Bates, F. S. *Macromolecules* **2006**, *39*, 6221−6228.
(38) Almdal, K.; Hillmyer, M. A.; Bates, F. S. *Macromolecules* **2002**, *35*, 7685−7691.
(39) Cavicchi, K. A.; Lodge, T. P. *Macromolecules* **2003**, *36*, 7158−7164.
(40) Pangborn, A. B.; Giardello, M. A.; Grubbs, R. H.; Rosen, R. K.; Timmers, F. J. *Organometallics* **1996**, *15*, 1518−1520.
(41) Ndoni, S.; Papadakis, C. M.; Bates, F. S.; Almdal, K. *Rev. Sci. Instrum.* **1995**, *66*, 1090−1095.
(42) Chu, J. H.; Rangarajan, P.; Adams, J. L.; Register, R. A. *Polymer* **1995**, *36*, 1569−1575.
(43) Zilliox, J. G.; Roovers, J. E. L.; Bywater, S. *Macromolecules* **1975**, *8*, 573−578.
(44) Gehlsen, M. D. Catalytic hydrogenation of polymers: synthesis and characterization of model polyolefins. Ph.D. Thesis, University of Minnesota, 1993.
(45) Fetters, L. J.; Lohse, D. J.; Richter, D.; Witten, T. A.; Zirkel, A. *Macromolecules* **1994**, *27*, 4639−4647.
(46) Epps, T. H., III; Bates, F. S. *Macromolecules* **2006**, *39*, 2676−2682.
(47) Hermel, T. J.; Wu, L.; Hahn, S. F.; Lodge, T. P.; Bates, F. S. *Macromolecules* **2002**, *35*, 4685−4689.
(48) Koppi, K. A. Shear oxidation of diblock copolymer melts. Ph.D. Thesis, University of Minnesota, 1993.
(49) Rosedale, J. H.; Bates, F. S. *Macromolecules* **1990**, *23*, 2329−2338.
(50) Schwahn, D.; Hahn, K.; Streib, J.; Springer, T. *J. Chem. Phys.* **1990**, *93*, 8383−8391.
(51) Scheffold, F.; Eiser, E.; Budkowski, A.; Steiner, U.; Klein, J.; Fetters, L. J. *J. Chem. Phys.* **1996**, *104*, 8786−8794.
(52) Hildebrand, J. H.; Scott, R. L. *The Solubility of Nonelectrolytes*, 3rd ed.; Van Nostrand-Reinhold: Princeton, NJ, 1950; p 475 ff.
(53) Graessley, W. W.; Krishnamoorti, R.; Balsara, N. P.; Fetters, L. J.; Lohse, D. J.; Schulz, D. N.; Sissano, J. A. *Macromolecules* **1993**, *26*, 1137−1143.
(54) Graessley, W. W.; Krishnamoorti, R.; Balsara, N. P.; Fetters, L. J.; Lohse, D. J.; Schulz, D. N.; Sissano, J. A. *Macromolecules* **1994**, *27*, 2574−2579.
(55) Krishnamoorti, R.; Graessley, W. W.; Balsara, N. P.; Lohse, D. J. *Macromolecules* **1994**, *27*, 3073−3081.
(56) Singh, C.; Schweizer, K. S. *Macromolecules* **1997**, *30*, 1490−1508.
(57) Schweizer, K. S.; Singh, C. *Macromolecules* **1995**, *28*, 2063−2080.
(58) Fredrickson, G. H.; Liu, A. J.; Bates, F. S. *Macromolecules* **1994**, *27*, 2503−2511.
(59) Dudowicz, J.; Freed, K. F. *Macromolecules* **1993**, *26*, 213−220.
(60) Freed, K. F.; Dudowicz, J. *Macromolecules* **1996**, *29*, 625−636.
(61) Dudowicz, J.; Freed, M. S.; Freed, K. F. *Macromolecules* **1991**, *24*, 5096−5111.
(62) Dudowicz, J.; Freed, K. F. *Macromolecules* **1991**, *24*, 5076−5095.

MA071132G